

## TWO-DIMENSIONAL RESONATORS WITH SMALL OPENINGS

G. R. BIGG and E. O. TUCK<sup>1</sup>

(Received 31 March 1981; revised 26 August 1981)

### Abstract

The acoustic response of a two-dimensional nearly-closed cavity to an excitation through a small opening is examined, using the method of matched asymptotic expansions. The Helmholtz mode of vibration is discussed using a low-frequency expansion of the velocity potential in the cavity interior. The variation in frequency and magnitude of the resonator response is explored, both for the Helmholtz and the natural-frequency modes.

### 1. Introduction

The acoustic response of a nearly-closed cavity to an excitation through a small opening contains peaks at frequencies close to the natural resonant frequencies of the fully-closed cavity, that is, at wavelengths comparable to, or smaller than, the dimensions of the cavity. In addition, there is a single low-frequency peak, unrelated to any non-trivial natural frequency of the cavity, and corresponding to a wavelength far in excess of the dimensions of the cavity. The cavity is said to be responding as a “Helmholtz resonator”, when the frequency is close to this peak. Although Helmholtz [2] discussed the nature of this resonance, Rayleigh ([8]; see also [9], Chapter 16) provided the first detailed analyses. These classical investigations are confined to three-dimensional cavities, these being of obvious acoustic relevance. The corresponding situation in two dimensions (that is, for a cavity consisting of an infinitely-long cylinder, pierced and communicating to the outside by a narrow infinitely-long slit) is of somewhat less acoustic interest, and has seldom been analysed in acoustics.

---

<sup>1</sup>Department of Applied Mathematics, University of Adelaide, Box 498, G.P.O., Adelaide, S.A. 5001.

© Copyright Australian Mathematical Society 1982

An indirect application of this two-dimensional configuration is to shallow-water theory in oceanography. For instance, the problem of harbour resonance can be reduced to solution of an acoustic-like problem in the horizontal plane, the coastline of the harbour playing the role of the cavity. Hence, some more recent studies ([5], [6], [7]) have considered this type of two-dimensional resonator.

In the present paper, we first treat a general class of small-opening problems in which the aim is to compute the response at all frequencies. That is, we obtain a theory which is asymptotically valid for small opening size (compared to both wavelength and cavity size), but which does not yet assume that the wavelength is far in excess of the cavity size. This theory is therefore, in principle, capable of predicting all peaks in the response, namely the Helmholtz peak and all of the peaks corresponding to natural frequencies of the fully-closed cavity.

The results depend on two specially-defined length parameters  $s$  and  $b$ , the former depending on the geometry of the opening, and the latter on the geometry of the cavity. The opening parameter  $s$  is independent of frequency, and is a generalization of that introduced by Tuck [10]. The present generalization is to allow the cavity wall in the neighbourhood of the opening to be nonplanar; specifically to allow the opening to be at the apex of a wedge-like region, of a general angle. Computation of  $s$  is quite straightforward, and examples are given for various types of opening geometries.

On the other hand, for general cavities, the computation of the cavity shape parameter  $b$  (which depends on frequency) is not at all straightforward. However, exact results for  $b$  are available for a special circular-sector cavity and are used to compute the response of this particular cavity as a function of frequency. These results are compared to those obtained by direct numerical solution of the boundary-value problem, using a boundary-integral-equation method similar to that of Lee ([3], [4]).

If we confine attention to the low-frequency (Helmholtz) mode, it is then not necessary to determine the cavity parameter  $b$  at all frequencies, and, in fact, all that is needed is its zero-frequency limit. The problem of determining  $b$  at zero frequency can be reduced to that of solving a Poisson equation in the closed cavity; a much simpler computational task. The resulting value of the logarithm of  $b$  is related to a parameter  $\mathfrak{N}$  introduced by Miles and Lee [7], and further examples of its computation are presented here.

Once  $b$  is known for any cavity, the response in the neighbourhood of the Helmholtz peak can be computed to a consistent order of approximation. This response is discussed for several cases. The variation of the over-all response with cavity shape, and the variations of response from one point in the cavity to another are discussed.

## 2. Problem formulation and numerical method

The mathematical task is to solve Helmholtz's equation

$$\nabla^2 \phi + k^2 \phi = 0 \quad (2.1)$$

for  $\phi = \phi(x, y)$  in a region  $R$  of the  $(x, y)$  plane bounded by a curve  $\Gamma$  across which there is no flow, that is,

$$\frac{\partial \phi}{\partial n} = 0 \quad \text{on } \Gamma. \quad (2.2)$$

The wavenumber  $k$  is a given positive constant. The only other boundary condition is at infinity, where  $\phi$  is prescribed, that is, as  $r = \sqrt{x^2 + y^2} \rightarrow \infty$ ,

$$\phi \rightarrow \phi_\infty(x, y) + e^{ikr} \cdot O(r^{-\frac{1}{2}}), \quad (2.3)$$

for some given function  $\phi_\infty$ . The order of the error term in (2.3) corresponds to an outgoing dispersing scattered signal, for  $e^{-i\omega t}$  time dependence.

The above is a quite general class of two-dimensional boundary-value problems. Our interest here is in the case when the boundary  $\Gamma$  is as in Figure 1, and can be decomposed into

$$\Gamma = \Gamma_E + \Gamma_C \quad (2.4)$$

$$= (\Gamma_E - \Gamma_0) + (\Gamma_C + \Gamma_0) \quad (2.5)$$

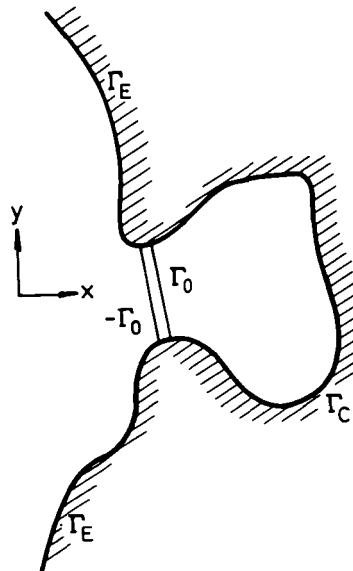


Figure 1. Sketch of boundary geometry.

where  $\Gamma_C$  is a cavity, and  $\Gamma_E$  an exterior boundary. Both  $\Gamma_E$  and  $\Gamma_C$  are open curves, but can be closed by addition and subtraction of an artificial boundary  $\Gamma_0$  across the cavity opening. We assume that  $\Gamma_0$  is chosen in such a way that  $\phi_\infty(x, y)$  is the *exact* solution of the boundary-value problem with  $\Gamma$  replaced by  $\Gamma_E - \Gamma_0$ . That is, our task is to compute the correction  $\phi - \phi_\infty$  introduced by distortion of the boundary  $\Gamma_E - \Gamma_0$ , due to introduction of the cavity  $\Gamma_C + \Gamma_0$ .

The example in which we are most interested is that when  $\Gamma_E - \Gamma_0$  is a straight line, and may be taken as the axis  $x = 0$ , and in which  $\phi_\infty$  corresponds to reflection of a plane wave incident at an angle  $\alpha$ , that is,

$$\phi_\infty = e^{iky \sin \alpha} \cos(kx \cos \alpha). \quad (2.6)$$

One method of solving the problem so formulated is to attack it numerically, using a boundary-integral-equation technique similar to that of Lee ([3], [4]). This approach involves use of the integral relations

$$\phi(\mathbf{x}) = -\frac{1}{2} i \int_{\Gamma_C + \Gamma_0} \left[ \phi(\mathbf{x}') \frac{\partial}{\partial n} H_0^{(1)}(kr') - H_0^{(1)}(kr') \frac{\partial \phi}{\partial n}(\mathbf{x}') \right] dl(\mathbf{x}') \quad (2.7)$$

for  $\mathbf{x} \in \Gamma_C + \Gamma_0$ , and

$$\phi(\mathbf{x}) = \phi_\infty(\mathbf{x}) + \frac{1}{2} i \int_{\Gamma_0} H_0^{(1)}(kr') \frac{\partial \phi}{\partial n}(\mathbf{x}') dl(\mathbf{x}') \quad (2.8)$$

for  $\mathbf{x} \in \Gamma_0$ , where  $H_0^{(1)}(kr')$  is the zeroth order Hankel function of the first kind, and

$$r' = |\mathbf{x} - \mathbf{x}'|. \quad (2.9)$$

Equations (2.7), (2.8) provide a pair of coupled integral equations to determine the unknown boundary values of  $\phi$  on  $\Gamma_C + \Gamma_0$  and  $\partial \phi / \partial n$  on  $\Gamma_0$ . A direct numerical solution procedure is to replace integration by summation in (2.7) and (2.8), giving a set of linear algebraic equations to solve for a vector of values of these unknown quantities. This procedure, while straightforward, is expensive in terms of computing time; inversion of large non-sparse matrices with complex elements being involved. The method is suitable therefore only for specific case studies, as of real harbours (Lee [4]), or as a benchmark.

The results of such a numerical computation will be used in Section 4 to validate the asymptotic approach to the resonance problem.

### 3. Flow through small openings

The matching procedures discussed in [10] are now adapted to the present problem. The opening geometry may be considered as a quite general one, as sketched in Figure 2. This general opening is a transition between an asymptotically-converging wedge of angle  $\theta_-$  on the left, and a corresponding diverging

wedge of angle  $\theta_+$  on the right. The length scale of the opening is a measure  $s$  of its linear size, and the requirement of smallness of the opening is that  $s$  be small compared to all other significant length scales, notably the wavelength  $2\pi/k$  and the linear size (say  $a$ ) of the cavity. Although  $s$  could be taken initially as any typical length dimension of the opening, for example, the minimum width  $w$ , our task is to determine a special measure  $s$ , that uniquely characterizes this opening geometry, as seen in its own far field.

Since  $ks$  is small, the flow in the opening is approximately incompressible, and thus we have to solve Laplace's equation for a flow through the opening. The behaviour of interest at infinity is that corresponding to a source-sink pair. Without loss of generality, we may normalize the net flux through the opening to unity, seeking therefore a scaled potential  $\bar{\phi}$  satisfying, as  $r \rightarrow \infty$ ,

$$\bar{\phi} \rightarrow \pm (\log r)/\theta_{\pm} + \text{constant} \quad \text{for } x \gtrless 0. \quad (3.1)$$

The "constant" in (3.1) does not necessarily take the same value when  $x \rightarrow +\infty$  as it does when  $x \rightarrow -\infty$ , and we now define our effective size  $s$  in terms of its change in value between the two infinities, writing instead of (3.1),

$$\bar{\phi} \mp [\log(r/s)]/\theta_{\pm} \rightarrow 0 \quad \text{as } x \rightarrow \pm \infty. \quad (3.2)$$

For any given opening geometry, our task is to solve  $\nabla^2 \bar{\phi} = 0$  for  $\bar{\phi}$ , subject to  $\partial \bar{\phi} / \partial n = 0$  on the opening boundaries, and the boundary condition (3.2) at infinity. As part of that solution process, the quantity  $s$ , having the dimensions of length, will be uniquely determined. This is a quite straightforward computational task, and  $s$  may therefore be treated as a known quantity.

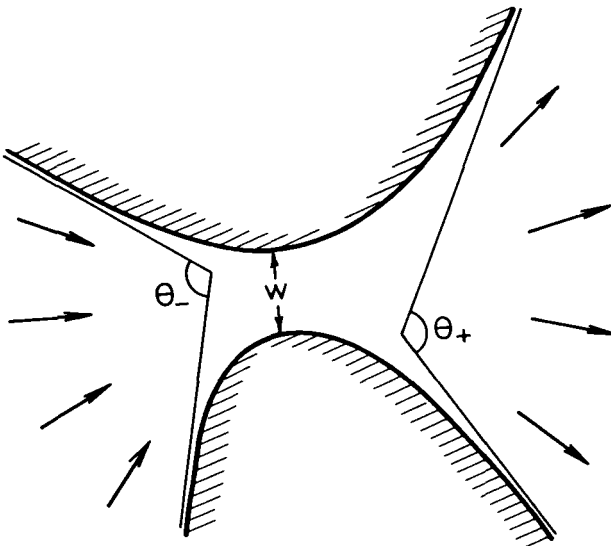


Figure 2 Sketch of opening geometry.

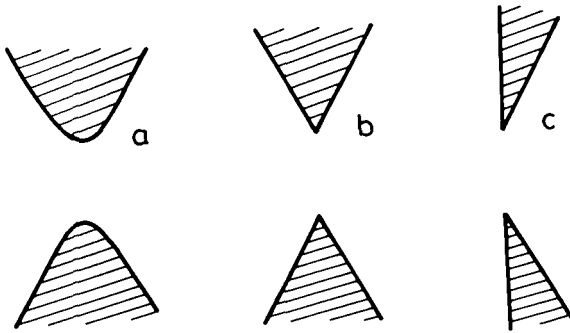


Figure 3. Special openings: (a) hyperbolic, (b) symmetric wedge, (c) wedge with  $\theta_- = \pi$ .

Most examples considered up to now and discussed in [10] have had  $\theta_+ = \theta_- = \pi$ , that is, they correspond to openings in a *plane* wall. In particular, if the opening is a sharp-edged slit of width  $w$ , in a plane wall of zero thickness, then  $s = \frac{1}{4}w$ .

In fact, the derivation (using elliptic coordinates) of this result in [10] generalizes immediately to that for an opening consisting of a pair of hyperbolas, as sketched in Figure 3a, which has  $\theta_+ = \theta_- < \pi$ . Now  $s$  is exactly equal to one quarter of the distance between the *foci* of the hyperbolae, that is, if  $w$  is the actual width at the throat,

$$s = \frac{w}{4 \sin(\theta_+/2)}. \quad (3.3)$$

A plot of  $s/w$  against  $\theta_+$  is shown in Figure 4 as the solid line.

Another case in which the effective size  $s$  can be determined at least semi-analytically, is that in which the boundaries are straight-edged wedges. A very general solution using a Schwartz-Christoffel mapping is presented in Appendix A. Figure 4 shows two examples of plots of  $s/w$  against  $\theta_+$ , for the case of openings with a plane of vertical symmetry. The dashed curve is for an opening (Figure 3b) which also has a plane of horizontal symmetry ( $\theta_+ = \theta_-$ ), and the chain-dotted curve is for  $\theta_- = \pi$ , that is, for an opening in a plane exterior wall, as in Figure 3c.

The results shown in Figure 4 indicate that the effective size of the opening is *increased* by decreasing the wall angles  $\theta_{\pm}$  from  $\pi$ . This is most easily explained in terms of the hyperbolic opening, for which the controlling parameter is the interfocal distance, which exceeds the actual throat width. The increase is not rapid, but by the time the angle  $\theta_+$  reaches  $90^\circ$ , a 100–150% increase in  $s$  is predicted. On the other hand, wall thickness *per se* tends to *decrease* the effective size (see [10]), providing  $\theta_+$  and  $\theta_-$  remain at  $180^\circ$ .

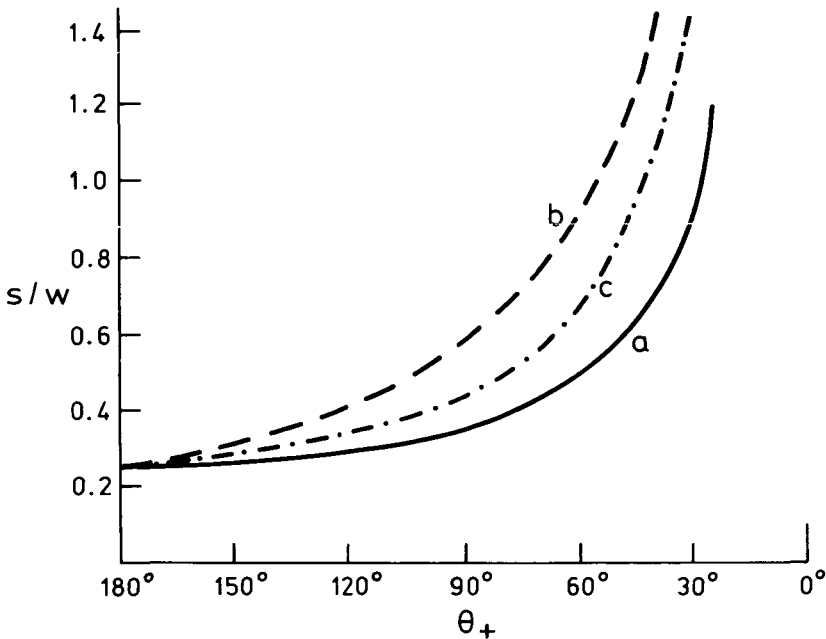


Figure 4. Effective size of openings of Figure 3.

We now consider the use of this canonical flow  $\bar{\phi}$  and its associated effective size parameter  $s$ , in the present acoustic problem. Although the above discussion allowed both  $\theta_-$  and  $\theta_+$  to be arbitrary, from now on for simplicity we shall restrict attention to the case  $\theta_- = \pi$ , that is, to an opening in an exterior plane wall, for which (2.6) prescribes the incident wave field  $\phi_\infty(x, y)$ . However, we allow  $\theta_+ < \pi$ , that is, the inside wall of the cavity near the opening need not be planar.

Now, in the limit as  $ks \rightarrow 0$ , the disturbance due to the cavity vanishes, and  $\phi \rightarrow \phi_\infty$ . The residual effect of the cavity, as seen in its own far field, must be that of an acoustic source. That is, if  $m$  is the strength of that source, we set in  $x < 0$ ,  $r \gg s$ ,

$$\phi = \phi_\infty - (1/4)imH_0^{(1)}(kr), \quad (3.4)$$

and seek to determine the quantity  $m$  by matching with the flow in the cavity, *via* the opening region.

In order to perform that matching, we let  $kr \rightarrow 0$  in (3.4), obtaining

$$\phi = \phi_\infty(0, 0) - (1/4)im[1 + (2i/\pi)\log((1/2)\bar{\gamma}kr)] + O(mk^2r^2\log kr), \quad (3.5)$$

where  $\log \bar{\gamma} = 0.577\dots$  is Euler's constant. The expression (3.5) must match with a boundary condition as  $x/s \rightarrow -\infty$  for a through-opening flow, and for that

purpose it can be re-written as

$$\phi \rightarrow \phi^0 + (m/2\pi)\log(r/s) \quad \text{as } x/s \rightarrow -\infty, \tag{3.6}$$

where the constant  $\phi^0$  is given by

$$\phi^0 = 1 - (1/4)im + (m/2\pi)\log((1/2)\bar{\gamma}ks), \tag{3.7}$$

noting from (2.6) that  $\phi_\infty(0, 0) = 1$ .

The solution for the incompressible flow through the opening is therefore (using (3.2) with  $\theta_- = \pi$ )

$$\phi(x, y) = \phi^0 - (m/2)\bar{\phi}(x, y), \tag{3.8}$$

where  $\bar{\phi}$  is the canonical potential defined above. Having solved for this opening flow, we may now proceed all the way into the cavity, by letting  $x/s \rightarrow +\infty$ , that is, again using (3.2),

$$\phi \rightarrow \phi^0 - \frac{m}{2\theta_+} \log\left(\frac{r}{s}\right) \quad \text{as } \frac{x}{s} \rightarrow +\infty. \tag{3.9}$$

Finally, we now match with a within-cavity solution, by observing that, if the opening size  $s$  is small compared to a typical measure  $a$  of the cavity size, the opening will appear to the cavity as a sink of strength  $\pi m/\theta_+$ , that is, (3.9) will provide a singularity condition as  $r/a \rightarrow 0$ . The potential in the cavity can therefore be written

$$\phi = - (\pi m/\theta_+) \phi_c(x, y), \tag{3.10}$$

where  $\phi_c$  satisfies (2.1) and (2.2) on the limiting (closed, as  $s \rightarrow 0$ ) boundary of the cavity, except that  $\phi_c$  behaves like a source of *unit* strength at the point on that boundary corresponding to the vanishing opening. That is, as  $r \rightarrow 0$ , we must have

$$\phi_c \rightarrow (2\pi)^{-1} \log r + \text{constant}. \tag{3.11}$$

The canonical potential  $\phi_c$  is thus uniquely determined, and, in particular, the “constant” in (3.11) is uniquely determined. We define a parameter  $b$  by choosing this constant to satisfy

$$\frac{\theta_+}{2\pi k^2 A} - \frac{1}{2\pi} \log b = \lim_{r \rightarrow 0} \left[ \phi_c - \frac{1}{2\pi} \log r \right], \tag{3.12}$$

where  $A$  is the cavity’s area. The parameter  $b$  measures the size of the cavity, as seen in the neighbourhood of its opening; it has the dimensions of a length, and may be expected to take values comparable to the cavity’s linear dimensions, that is,  $b = O(A^{1/2})$ . For the moment, let us assume that  $\phi_c$ , and hence  $b$ , can be determined for any given cavity.

Now, as  $r \rightarrow 0$ ,

$$\phi \rightarrow -\frac{\pi m}{\theta_+} \left[ \frac{1}{2\pi} \log \frac{r}{b} \right] - \frac{m}{2k^2 A}, \quad (3.13)$$

which matches with (3.9) if

$$\phi^0 + \frac{m}{2\theta_+} \log s = \frac{m}{2\theta_+} \log b - \frac{m}{2k^2 A}. \quad (3.14)$$

Upon use of (3.7) for  $\phi^0$ , we obtain the required formula for the source strength  $m$ , namely

$$m^{-1} = -\frac{1}{2k^2 A} - \frac{1}{2\pi} \log \left( \frac{1}{2} \bar{\gamma} k s \right) + \frac{1}{2\theta_+} \log(b/s) + \frac{1}{4} i. \quad (3.15)$$

The small-gap theory is now complete, with the determination of the source strength  $m$ . In summary, the exterior-region potential is given by (3.4), the opening-region potential by (3.8), and the cavity-region potential by (3.10). As inputs, we need the canonical potentials  $\bar{\phi}$  in the opening, and  $\phi_c$  in the cavity. Associated with  $\bar{\phi}$  is a single parameter  $s$ , with dimensions typical of the opening. Associated with  $\phi_c$  is a single parameter  $b$ , with dimensions typical of the cavity. Since  $\bar{\phi}$  satisfies Laplace's equation,  $s$  is frequency-independent, but since  $\phi_c$  satisfies Helmholtz's equation, we must expect  $b$  to depend on frequency.

It is worth reiterating that the only approximation made to this point is that the effective size  $s$  of the gap is small compared with all other relevant length scales. We have not yet assumed that the cavity size  $a$  is small compared to the wavelength. In particular, the error in an expression such as (3.15) is at most a factor of order  $1 + O(ks, s/a)$ .

#### 4. Results for large circular-sector cavities

The task of determining the canonical cavity potential  $\phi_c(x, y)$ , satisfying (2.1), (2.2) and (3.11) is still a quite difficult one, and exact analytic solutions are few. One case in which a solution can be written down, is that for a cavity consisting of a sector of a circle, with the opening at the apex. That is, if  $(r, \theta)$  are polar coordinates centred at the location of the opening, the boundary consists of a circular arc  $r = a$  and radial lines  $\theta = \pm \frac{1}{2}\theta_+$ , and has area  $A = \frac{1}{2}\theta_+ a^2$ . In particular, if  $\theta_+ = \pi$ , the cavity is semi-circular, with the opening at the centre of the diameter.

It is clear then that all conditions are satisfied if

$$4\phi_c = Y_0(kr) - \frac{Y'_0(ka)}{J'_0(ka)} J_0(kr), \quad (4.1)$$

and the parameter  $b$  is given by

$$\log\left(\frac{1}{2}\bar{\gamma}kb\right) = \frac{2}{k^2a^2} + \frac{\pi}{2} \frac{Y'_0(ka)}{J'_0(ka)}. \tag{4.2}$$

The source strength  $m$  can now be evaluated using (3.15), and hence the value of the potential on the cavity wall  $r = a$  is

$$\begin{aligned} \phi_c &= \frac{m}{2ka\theta_+ J'_0(ka)} \\ &= \frac{2}{\pi ka} \left[ Y'_0(ka) + J'_0(ka) \left\{ \frac{\theta_+}{\pi} i - \frac{2}{\pi} \left( 1 + \frac{\theta_+}{\pi} \right) \log\left(\frac{1}{2}\bar{\gamma}ks\right) \right\} \right]^{-1}. \end{aligned} \tag{4.3}$$

An illustrative plot of  $|\phi|$  against  $ka$  is given in Figure 5, for the case of a semi-circular cavity ( $\theta_+ = \pi$ ) with  $s/a = 0.05$ .

Peaks in the response  $|\phi|$  in the cavity occur whenever the quantity inside the square brackets of (4.3) is small. Since  $ks$  is small, that is,  $-\log(\frac{1}{2}\bar{\gamma}ks)$  is large, this quantity is usually dominated by its second term, and hence peaks occur when  $J'_0(ka) = 0$ . This is just another way of saying that, when the opening is small, the cavity behaves almost as if it were closed, and the condition  $J'_0(ka) = 0$  precisely determines those natural eigenmodes of the closed cavity without  $\theta$ -dependence. This cavity can also support modes with  $\theta$ -dependence, but these possess a node at  $r = 0$ , and hence are not excited through a vanishingly small opening there.

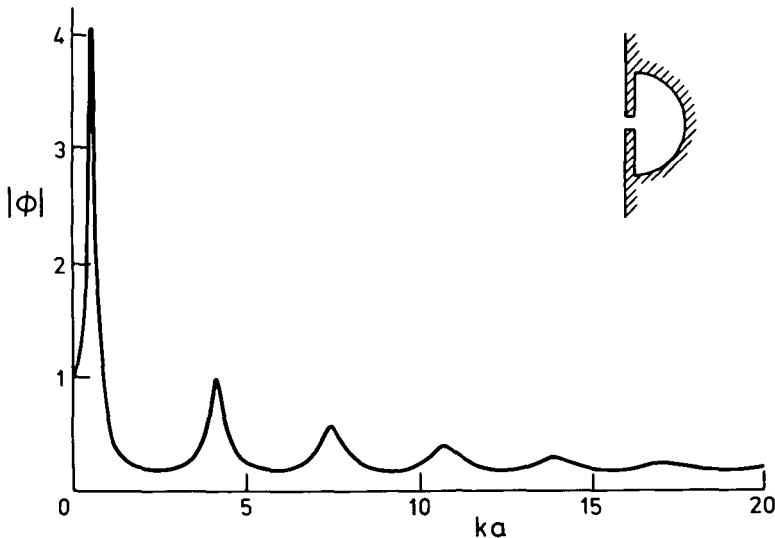


Figure 5. Response of semi-circular cavity of radius  $a$  and opening of effective size  $s = 0.05a$ , computed by asymptotic theory for small  $s/a$ , and evaluated on the curved boundary.

However, the square bracket in (4.3) can also become small when  $ka$  is small, because then the leading term  $Y_0'(ka)$  becomes large and can cancel the second term. This defines the Helmholtz mode, the first and highest peak in Figure 5. This mode will be discussed further in the following section, for general cavities. In the present case, we note the following expansion of the "exact" cavity potential  $\phi_c$  as  $ka \rightarrow 0$ , namely

$$\phi_c = \frac{1}{\pi k^2 a^2} + \frac{1}{2\pi} \left[ \log \frac{r}{a} - \frac{1}{2} \frac{r^2}{a^2} + \frac{3}{4} \right] - \frac{k^2 a^2}{8\pi} \left[ \frac{r^2}{a^2} \log \frac{r}{a} - \frac{1}{4} \frac{r^2}{a^2} - \frac{1}{8} \right] + O(k^4 a^4), \quad (4.4)$$

which implies

$$b/a = e^{-3/4} + O(k^2 a^2). \quad (4.5)$$

The corresponding formula for the source strength  $m$  follows directly from (3.15), and the small- $ka$  expansion for the response on the cavity wall  $r = a$  can then be written

$$\phi = \frac{1 + \frac{1}{8} k^2 a^2 + O(k^4 a^4)}{1 - 2k^2 A \left[ -\frac{1}{2\pi} \log \left( \frac{1}{2} \bar{\gamma} ks \right) + \frac{1}{2\theta_+} \log \frac{a}{s} - \frac{3}{8\theta_+} + \frac{1}{4} i \right] + O(k^4 a^4)}. \quad (4.6)$$

Equation (4.6) can also be obtained by a sufficiently-careful direct small- $ka$  expansion of equation (4.3). The difficulty occurs because we must assume  $-\log(\frac{1}{2}s)$  to be a very large quantity, indeed at least as large as  $(ka)^{-2}$ . This is necessary if we are to be able to discuss the Helmholtz resonance mode, in which substantial cancellation must occur between the leading-order terms in the denominator of (4.6). The advantage of the particular form adopted for (4.6) (as the ratio between two separate expansions with respect to  $ka$ ), is that the error terms quoted as  $O(k^4 a^4)$  for both numerator and denominator are errors resulting *only* from expansions of  $\phi_c$ , and are completely independent of the opening parameter  $s$ .

The accuracy of formula (4.3) may be checked by comparison with computations made for a semi-circular cavity, using the numerical method outlined in Section 2. For that purpose, the cavity was divided into a maximum of 80 segments. That is, at most 30 segments were needed on each half of the actual symmetric cavity boundary  $\Gamma_c$ , and 10 on each half of the (straight) artificial boundary  $\Gamma_0$  across the opening. About 3-figure accuracy was always achievable (even close to the peaks) with this coarse discretization, since  $\phi$  varies only slowly

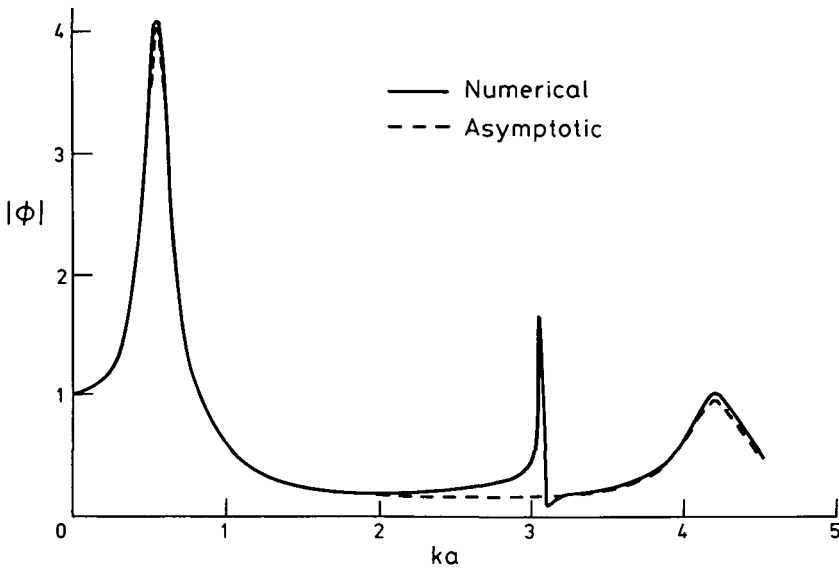


Figure 6. Comparison of numerical and asymptotic results for semi-circular cavity at  $s/a = 0.05$ .

around the boundary, except at the junction between  $\Gamma_c$  and  $\Gamma_0$ . Segment distribution was generally uniform, but with a certain amount of accumulation near that junction.

The output potential  $\phi$  around the boundary can be used to provide  $\phi$  at any point in the cavity, as long as the cavity is not too narrow. Thus a complete description of the field in the cavity may be obtained.

The numerical results for  $s/a < .02$  are in agreement, to 2 or 3 figures, for all tested  $k$ , with the asymptotic results using (4.3). Even for considerably larger  $s$ , the approximation of the Helmholtz and radially-symmetric natural modes by (4.3) is very good.

However, as the cavity mouth increases in size, the  $\theta$ -dependent modes mentioned above begin to appear. In Figure 6, the velocity potential at  $(a, 0)$  is shown for  $s/a = 0.05$ , to illustrate this last-mentioned phenomenon. The two plots are in excellent agreement everywhere, except in the vicinity of  $ka \approx 3.05$ . This is the resonant frequency of a  $\theta$ -dependent mode, with two nodal lines  $\theta = \pm\pi/4$ , intersecting at right angles at  $r = 0$ .

Having confirmed the good agreement of (4.3) with an independent numerical solution of the problem, we now consider the effect of the opening size  $s$  on the response curves.

In Figure 7, the first two resonance peaks for a semicircle are shown, for several  $s$  values, computed from (4.3). As expected from this equation and (4.6), a

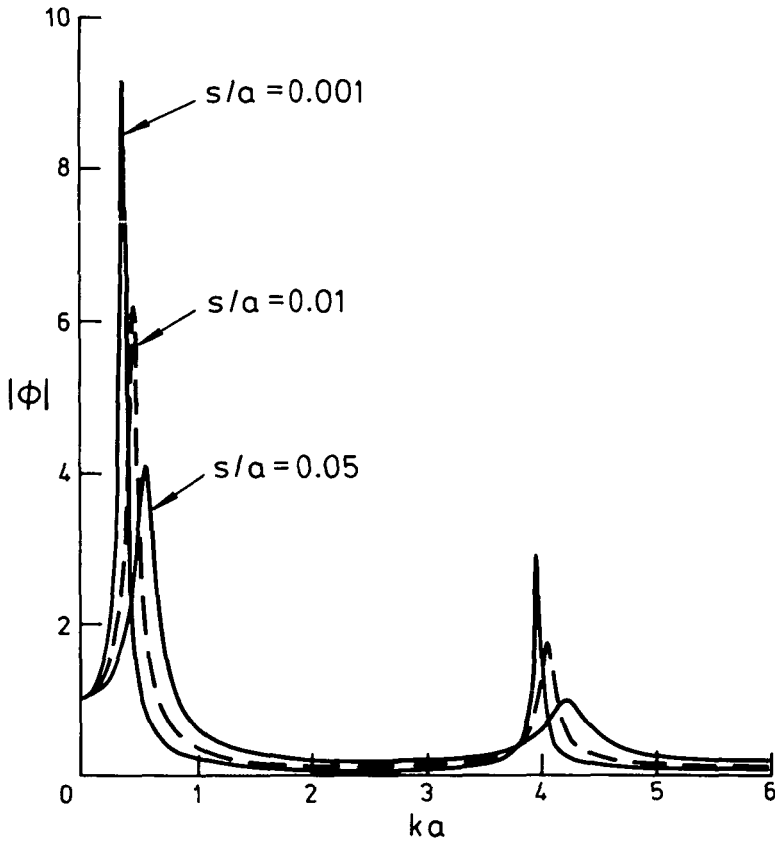


Figure 7. Variation in response of semi-circular cavity with opening size  $s$ .

reduction in the size  $s$  of the opening shifts the Helmholtz peak to a somewhat smaller frequency  $k$ , and increases the peak amplitude dramatically. It is also to be noted that, as  $s$  decreases, the position of the first natural frequency also changes, its bandwidth reduces and its maximum amplitude increases. However, the quantitative nature of these changes differs from the alterations to the Helmholtz peak [5].

The effect of the variation of the interior cavity angle  $\theta_+$  near the opening is also of interest. We illustrate this in Figure 8 for  $\theta_+ = 90^\circ$ . As  $\theta_+$  is decreased, the magnitude of the response increases. This indicates that the energy entering the cavity is not decreasing as quickly as the cavity area, which is consistent with the expression for  $m$  given in (3.15). Figure 8 also shows the position of the resonance altering slightly, again consistent with (4.3).

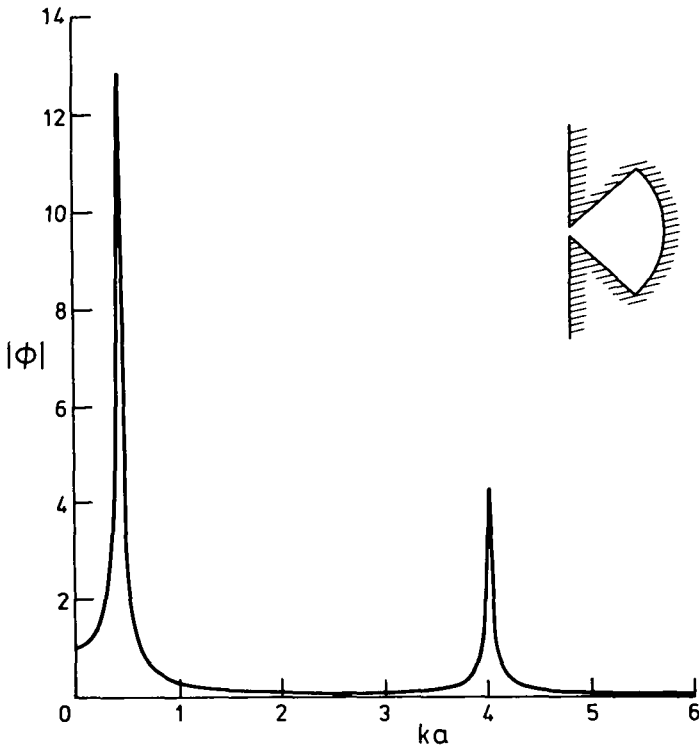


Figure 8. Response of 90° circular sector cavity, compare with the curve in Figure 7 for  $s/a = .001$ .

### 5. Solution for small cavities of general shape

Although the task of determining the cavity potential  $\phi_c$  is formidable in general, for the Helmholtz mode we are really only interested in the small- $ka$  expansion of  $\phi_c$ , as typified by equation (4.4) for the circular-sector cavity, where  $a = O(A^{1/2})$ . Using (4.4) as a guide, we therefore attempt to find a power series in  $k^2a^2$  of the form

$$\phi_c = \phi_0 + \phi_1 + \phi_2 + \dots \tag{5.1}$$

where we expect  $\phi_0 = O(k^{-2}a^{-2})$ ,  $\phi_1 = O(1)$ ,  $\phi_2 = O(k^2a^2)$  and so on.

In fact, we expect that the leading term  $\phi_0$  is *constant* throughout the cavity. This is anticipated, not only by analogy with (4.4), but also by physical arguments, since this corresponds to uniform compression of the whole cavity, the only possible form of motion in the low-frequency limit  $k \rightarrow 0$ .

Now if the series (5.1) is substituted into the Helmholtz equation (2.1), there results a sequence of Poisson equations for  $\phi_1, \phi_2, \dots$ , that is,

$$\nabla^2 \phi_1 = -k^2 \phi_0, \quad (5.2)$$

$$\nabla^2 \phi_2 = -k^2 \phi_1, \quad (5.3)$$

and so on. Similarly, the wall boundary condition (2.2) implies that

$$\frac{\partial \phi_1}{\partial n} = 0, \quad \frac{\partial \phi_2}{\partial n} = 0 \quad \text{and so on.} \quad (5.4)$$

An important set of integral relations follows if we integrate both sides of (5.2) and (5.3) over the cavity  $R$ , with boundary  $\Gamma_C + \Gamma_0$ . Thus

$$\iint_R \nabla^2 \phi_1 \, dx \, dy = -k^2 \phi_0 A = \oint_{\Gamma_C + \Gamma_0} \partial \phi_1 / \partial n \, dl \quad (5.5)$$

is the net flux of  $\phi_1$  produced by the constant forcing term on the right. But since  $\partial \phi_1 / \partial n = 0$  on the actual (open) cavity boundary  $\Gamma_C$ , the only contribution to the line integral on the right of (5.5) comes from the flow through the opening  $\Gamma_0$ , which has shrunk to a point. The opening is represented now by a source of unit strength in a sector of angle  $\theta_+$ , which therefore produces net (outgoing) flux  $-\theta_+ / (2\pi)$ . That is,

$$-k^2 \phi_0 A = -\theta_+ / (2\pi),$$

which determines the leading term in the series (5.1) as

$$\phi_0 = \theta_+ / (2\pi k^2 A). \quad (5.6)$$

Since the term  $\phi_1$  in (5.1) already accounts fully for the unit-source character of  $\phi_c$ , further terms  $\phi_2, \phi_3, \dots$  in the series do not produce any net flux through the opening. Hence, for example,

$$\iint_R \nabla^2 \phi_2 \, dx \, dy = -k^2 \iint_R \phi_1 \, dx \, dy = \oint_{\Gamma_C + \Gamma_0} \partial \phi_2 / \partial n \, dl = 0.$$

The resulting integral condition,

$$\iint_R \phi_1 \, dx \, dy = 0, \quad (5.7)$$

is a normalization for the potential  $\phi_1$  that ultimately determines the cavity parameter  $b$ . The process of solving (5.2) to determine  $\phi_1$ , and hence the parameter  $b$ , is illustrated in the following section, but for the moment we assume  $b$  is a known quantity, of the order of  $a = O(A^{1/2})$ , and subject to a relative error of  $O(k^2 a^2)$ .

Equation (3.15) now gives the source strength  $m$ , with error  $O(k^2a^2)$ , and hence the potential in the cavity is (from (3.10)),

$$\phi = (\pi m / \theta_+) [\theta_+ / (2\pi k^2 A) + \phi_1],$$

that is

$$\phi / \phi_m = 1 + (2k^2 A \pi / \theta_+) \phi_1(x, y) + O(k^4 a^4), \tag{5.8}$$

where

$$m = -2k^2 A \phi_m, \tag{5.9}$$

that is,

$$\begin{aligned} \phi_m^{-1} = 1 - 2k^2 A \left[ - (2\pi)^{-1} \log\left(\left(\frac{1}{2}\right) \bar{\gamma} k s\right) + (1 / (2\theta_+)) \log b / s + i / 4 \right] \\ + O(k^4 a^4). \end{aligned} \tag{5.10}$$

Equation (5.8) determines the flow everywhere in the cavity except near the opening, where  $\phi_1$  is singular. For the flow in the neighbourhood of the opening, we use (3.8) to give

$$\phi / \phi_m = 1 - (k^2 A / \theta_+) \log(b/s) + k^2 A \bar{\phi}(x, y) + O(k^4 a^4), \tag{5.11}$$

where  $\phi_m$  is again given by (5.10).

Both equations (5.8) and (5.11) predict only second-order spatial effects on the response; that is, neglecting the term  $(2\pi / \theta_+) k^2 A \phi_1(x, y)$  in (5.8) indicates that  $\phi$  is almost constant (and equal to  $\phi_m$ ) in the cavity. Similarly, neglecting the term  $k^2 A \bar{\phi}(x, y)$  in (5.11) predicts a constant response in the opening. However, these constant values are not quite equal to each other, and we predict that

$$\frac{\phi_{\text{opening}}}{\phi_{\text{cavity}}} = 1 - \frac{k^2 A}{\theta_+} \log\left(\frac{b}{s}\right) + O(k^2 a^2). \tag{5.12}$$

This ratio is significantly less than unity, since  $-\log(b/s)$  is large.

An approach giving results similar to this theory is that of Miles and Lee [7]. Using variational methods, they define a parameter  $\mathfrak{N}$ , found from solution of a Poisson equation, which incorporates the parameter  $s$ , and the zero frequency limit of  $b$ . In fact, it appears that, in our notation,

$$\mathfrak{N} = (1/\pi) \log(b/s). \tag{5.13}$$

Thus, both the cavity and the aperture geometry are involved in the specification of the parameter  $\mathfrak{N}$ . Miles and Lee have some difficulty in defining and computing  $\mathfrak{N}$ , in the general case, and construct a lower bound which seems to approximate their parameter adequately. The approach we have discussed in the preceding sections, however, differentiates between the opening and the cavity

geometries, and thus indicates separately the relative importance of these quantities in the final solution.

The importance of the analysis in the present section is that it enables coverage of the frequency regime in which the Helmholtz resonance occurs. Such a resonance corresponds to large magnitudes for  $\phi_m^{-1}$  in equation (5.10). Since the imaginary part of  $\phi_m^{-1}$  is small and provides damping, such a resonance will occur near to wavenumbers  $k$  such that the real part of  $\phi_m^{-1}$  vanishes, that is, where

$$2k^2A = \left( - (2\pi)^{-1} \log\left(\left(\frac{1}{2}\right) \bar{\gamma} ks\right) + (1/(2\theta_+)) \log(b/s) \right)^{-1}. \tag{5.14}$$

Although (5.14) is a transcendental equation for the resonant wavenumber  $k$ , it is clear that the order of magnitude of this  $k$  is given by

$$ka = O(\log(b/s))^{-1/2}. \tag{5.15}$$

Hence, in this range of wavenumbers, the error in the present results is a factor of the order of  $1 + O(\log(b/s))^{-2}$ .

### 6. The cavity shape parameter $b$ for special small cavities

The computational task for small  $ka$  reduces to that of solving the Poisson equation (from (5.2) and (5.6))

$$\nabla^2 \phi_1 = -\theta_+ / (2\pi A), \tag{6.1}$$

in  $R$ , subject to (5.4), that is,

$$\partial \phi_1 / \partial n = 0 \quad \text{on } \Gamma_C \tag{6.2}$$

and, from (3.11) and (3.12),

$$\phi_1 - (2\pi)^{-1} \log(r/b) \rightarrow 0 \quad \text{as } r \rightarrow 0, \tag{6.3}$$

where  $r = 0$  defines the vanishingly-small opening on the wall of the cavity. The system (6.1), (6.2) and (6.3) possesses a solution for any value of the constant  $b$ , but the value of  $b$  is rendered unique by the normalization condition (5.7).

The following symmetry considerations apply to the parameter  $b$ . Suppose the cavity  $R$  under consideration possesses symmetry about the  $x$ -axis, and the opening is at the origin. If we now place a rigid wall along this  $x$ -axis and consider only one of the identical chambers  $R^\pm$  created by this action, this half-chamber has the same shape parameter  $b$  as the original full cavity. This is because:

- (i) The ratio  $\theta_+ / A$  in (6.1) is unchanged, the new opening lying in the corner of angle  $\pi/2$ ,
- (ii) the potential  $\phi_1$ , for  $R$  will also satisfy all required conditions for  $R^+$ , and

(iii) the normalization integral (5.7) over  $R^+$  is just half that over  $R$ , and therefore also vanishes.

Now suppose we create a third cavity  $R^*$ , whose axis of symmetry is the  $y$ -axis, by reflecting  $R^+$  with respect to that axis. Now by the same arguments,  $R^*$  has the same value of  $b$  as does  $R^+$ , and therefore the same value of  $b$  as does the original cavity  $R$ .

The simplest case of computation of  $b$  is for the circular sector cavity already discussed. Now an appropriate solution of the Poisson equation (6.1) is

$$\phi_1 = \frac{1}{2\pi} \log \frac{r}{b} - \frac{\theta_+}{8\pi A} r^2 \tag{6.4}$$

and if the integral in (5.7) is evaluated, we find  $b = ae^{-3/4}$ , as in equation (4.5). The expression (6.4) also agrees with the  $O(1)$  term in the expansion (4.4) of  $\phi_c$  in powers of  $ka$ .

If the cavity consists of a *complete* circle  $r = 2a \cos \theta$ , then  $\theta_+ = \pi$ , and a solution of (6.1) subject to (6.2) and (6.3) can be written

$$\phi_1 = \frac{1}{2\pi} \log \left( \frac{r}{b} \right) - \frac{r^2 - 2ar \cos \theta}{8\pi a^2} \tag{6.5}$$

which satisfies (5.7) if

$$b = ae^{1/8}. \tag{6.6}$$

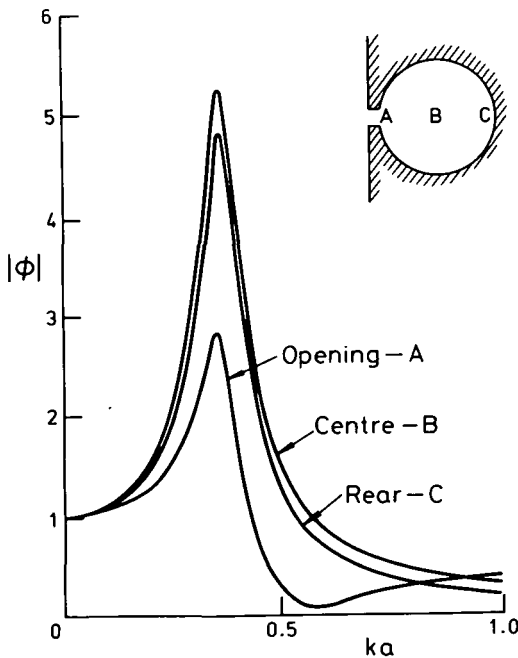


Figure 9. Helmholtz response of a complete circular cavity of radius  $a$  at  $s/a = 0.05$ , for various positions within the cavity.

This circular cavity can be used to illustrate dependence of the response on position in the cavity. Figure 9 shows  $|\phi|$  at  $s/a = 0.05$ , computed from (5.8), using (6.5) to give  $\phi_1$ , for two positions within the cavity. This figure shows the essential spatial invariance for non-resonant frequencies, but a significant variation in the magnitude (not the frequency) of the Helmholtz peak. The response in the opening itself is also shown, using (5.11) with  $\bar{\phi}$  taken as zero, indicating, as predicted by (5.12), a significantly reduced response at all frequencies.

Equation (6.6) can be generalized to

$$\phi_1 = (2\pi)^{-1} \log(r/b) - r^2/(8A) + \Phi \tag{6.7}$$

where  $\Phi$  is any solution of Laplace's equation vanishing at  $r = 0$ . In this way, for a given  $\Phi$ , one can construct inverse solutions of the present problem, the cavity's boundary curve  $r = r(\theta)$  being determined by solving the ordinary differential equation

$$\frac{dr}{d\theta} = r^2 \frac{\phi_{1r}(r, \theta)}{\phi_{1\theta}(r, \theta)} \tag{6.8}$$

which follows from (6.2). For example, if

$$\Phi = -(\lambda/(4\pi a^2))r^2 \cos 2\theta \tag{6.9}$$

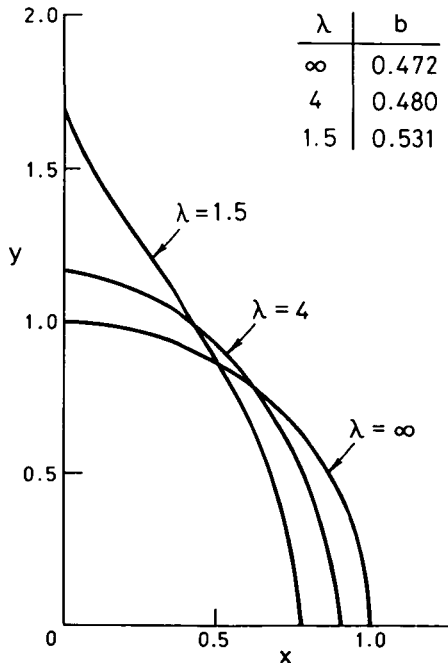


Figure 10. A class of inversely-determined cavity shapes with known cavity parameter  $b$ .

for some constant  $\lambda$ , we find

$$\lambda r^2 \sin 2\theta = 2a^2 \tan^{-\lambda} \theta \int_0^\theta \tan^\lambda \theta' d\theta'. \tag{6.10}$$

Figure 10 shows the cavity shapes and corresponding values of  $b$  for various  $\lambda$ . The symmetry property discussed above applies to these results.

Finally, a solution for a rectangular cavity can be constructed in the form

$$\begin{aligned} \phi_1 = & \frac{1}{4\pi} \log \left[ \sinh^2 \frac{\pi x}{2h} + \sin^2 \frac{\pi y}{2h} \right] \\ & - \frac{x^2}{8hL} + \frac{1}{4hL} \sum_{n=0}^{\infty} a_n \cosh \frac{n\pi x}{h} \cos \frac{n\pi y}{h} \end{aligned} \tag{6.11}$$

for suitable real coefficients  $a_n$ ,  $n = 0, 1, 2, \dots$ . The rectangle has length  $L$  and breadth  $2h$ , the opening being located at the centre  $(x, y) = (0, 0)$  of one of the sides of breadth  $2h$ . The expression (6.11) satisfies (6.3) if

$$\sum_{n=0}^{\infty} a_n = \frac{2Lh}{\pi} \log \left( \frac{2h}{\pi b} \right). \tag{6.12}$$

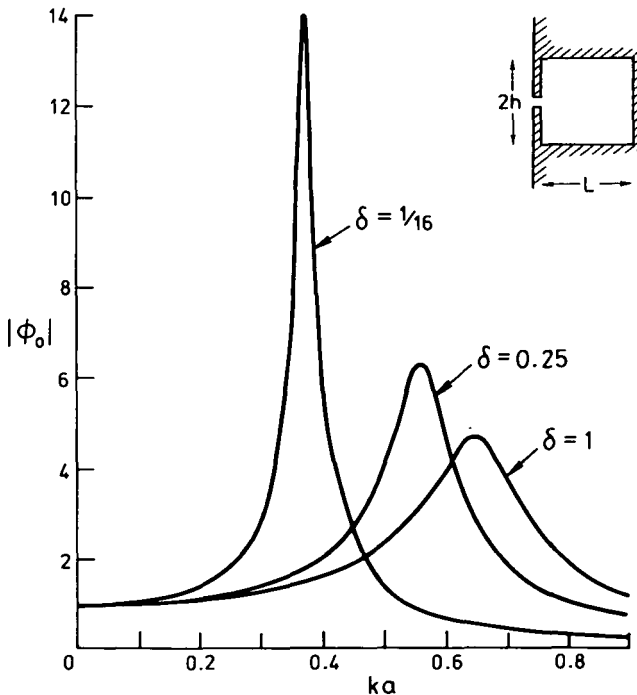


Figure 11. Helmholtz response of rectangular cavities of constant area  $A$ , at constant opening size  $s/A^{1/2} = 0.025$ , for various aspect ratios  $\delta = 2h/L$ .

The remaining boundary condition,  $\partial\phi_1/\partial n = 0$  on  $x = L$  yields formulae for  $a_n$ ,  $n = 1, 2, \dots$ , as coefficients in a Fourier-cosine series. The remaining coefficient  $a_0$  (and hence  $b$  from (6.12)) is determined by the normalization integral (5.7). The final expression for  $b$  is quite complicated, but can be written as a rapidly-converging double sum (see Appendix B).

The results for the rectangular cavity can be used to illustrate dependence of the Helmholtz resonance on cavity shape, *via* the aspect ratio  $\delta = 2h/L$ , holding the area  $A = 2hL$  fixed. Figure 11 shows  $|\phi_m|$  plotted against  $kA^{1/2}$  for various  $\delta$ , at  $s/A^{1/2} = 0.025$ . As indicated in Section 5,  $\phi_m$  measures the mean response everywhere in the cavity, with relative error  $O(k^2A)$ ; it in fact corresponds to the value of  $\phi$  near the side furthest from the opening.

The most striking feature in Figure 11 is the significant variation with  $\delta$  in both position and magnitude of the Helmholtz resonance peak. Thus, cavity shape plays an important role in determining the Helmholtz resonance; this is the opposite conclusion to that of classical theory for three dimensional cavities (see Tuck [10]). Two dimensional resonators thus have quite different properties, unless second-order effects in three dimensions are larger than expected.

The symmetry property demonstrated at the beginning of this section is found with rectangular cavities. The result is that cavities with an aspect ratio  $\delta$  have the same response curves as those with an aspect ratio of  $4/\delta$ . For example a square with the opening in the middle of a side has the same response characteristics as a rectangle of aspect ratio  $\delta = 4$ , with the opening in the middle of the long side.

Potentials in other cavities may be found by separation of variables (as for the rectangle), or by conformally mapping the region of interest to one for which solutions are already known, or to a half-plane.

## 7. Conclusion

In this paper, we have obtained asymptotic expansions for the response of cavities of arbitrary shape with small openings, also of arbitrary shape. The effect of the boundary geometry is obtained *via* two independent length parameters, one related to the opening and the other to the cavity.

The opening parameter  $s$  is well known to be an important influence on the response of the cavity, and was in effect already used by Rayleigh in his analysis of the Helmholtz resonator. However, it is conventional to assume that, at least for the Helmholtz mode, the shape of the cavity is not important, only its net area  $A$  influencing the response. Our results, being expressed in terms of a uniquely-defined cavity-shape parameter  $b$ , are capable of testing this assumption.

In fact, if  $b$  is allowed to vary, for cavities of constant area  $A$  and constant opening parameter  $s$ , the variation in response is usually small, but sometimes

significant, especially in the immediate neighbourhood of resonance. Quite large variations are obtained, for example, by varying the aspect ratio of a rectangular cavity from unity through values as high as 16.

In addition, our results show how the response varies from point to point around the boundary, whereas the classical analysis for a Helmholtz resonator predicts a uniform response. Again the variation is not large except near resonance, unless the observation point lies near the opening, when significantly lower responses occur at all frequencies.

### Appendix A: Determination of effective size of wedge-like openings

Our task is to solve Laplace's equation in a region with boundaries given as in Figure 12. The boundaries consist of two wedges, with angles  $\alpha\pi$  and  $\beta\pi$ , the vertices being located at points  $D$  and  $H$  respectively. Without loss of generality,

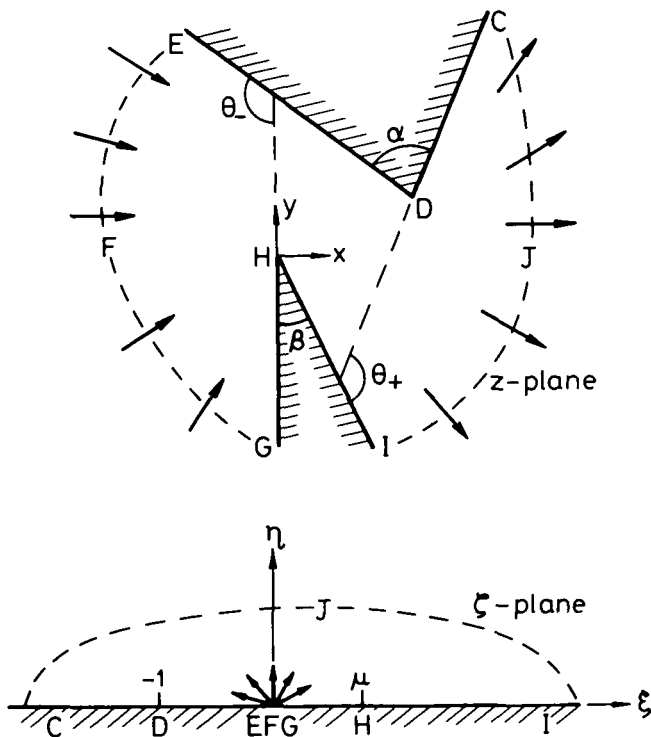


Figure 12. Conformal mapping of wedge-like openings.

we may fix the location of  $H$  as the origin in the complex  $z = x + iy$  plane, and also fix as vertical, the left edge of the wedge with corner at  $H$ . The angles  $\theta_-$  and  $\theta_+$  are as in the text, and necessarily

$$\theta_+ + \theta_- + \alpha\pi + \beta_\pi = 2\pi. \tag{A1}$$

It is convenient to set  $\theta_- = \gamma\pi$ .

The problem is solved by a Schwartz-Christoffel mapping to the upper half  $\eta \geq 0$  of the  $\zeta = \xi + i\eta$  plane, namely

$$\frac{dz}{d\zeta} = -ie^{i\beta\pi}\zeta^{-\gamma-1}(\zeta + 1)^{1-\alpha}(\zeta - \mu)^{1-\beta}, \tag{A2}$$

for some parameter  $\mu$ . The corner points  $D$  and  $H$  are mapped from the points  $\zeta = -1, \mu$  respectively. The overall length scale in this problem is arbitrarily determined by the fact that the constant multiplier in (A2) has unit magnitude.

The appropriate integral of (A2), satisfying  $z(\mu) = 0$ , is (for  $\zeta = \xi + i0$  and  $\xi < \mu$ )

$$z = -\frac{i\mu^{-1-\beta}}{\gamma}(\xi^{-\gamma} - \mu^{-\gamma}) + i\int_{\mu}^{\xi} t^{-\gamma-1}[(t + 1)^{1-\alpha}(\mu - t)^{1-\beta} - \mu^{1-\beta}] dt. \tag{A3}$$

Our main interest is in the location of the corner point  $D$ , which can be written as

$$z(-1) = i\mu^{1-\beta}[\mu^{-\gamma}F(\alpha, \beta, \mu) - e^{-i\gamma\pi}F(\beta, \alpha, 1/\mu)], \tag{A4}$$

where

$$F(\alpha, \beta, \mu) = 1/\gamma - \int_0^1 t^{-\gamma-1}[(1 + \mu t)^{1-\alpha}(1 - t)^{1-\beta} - 1] dt. \tag{A5}$$

There is no difficulty in numerical integration to determine the function  $F$  in (A5), and hence the coordinates of the point  $D$ . The method used here is to make the preliminary change of variable  $t = \tau^{1/(1-\gamma)}$ , which eliminates the algebraic singularity at  $t = 0$ , and then use the mid-point rule. In the particular case  $\mu = 1, \alpha = \beta$ , the function  $F$  reduces to a Beta-function, namely

$$F(\alpha, \alpha, 1) = ((1 - \alpha)/\gamma)B(1 - \frac{1}{2}\gamma, 1 - \alpha). \tag{A6}$$

This special case yields an opening with symmetry about a line through the mid-point of  $HD$ .

The flow problem is solved in the  $\zeta$ -plane by placing a source at the origin. That is, the complex potential is given by

$$\bar{f} = \bar{\phi} + i\bar{\psi} = (1/\pi)\log \zeta + K, \tag{A7}$$

for some constant  $K$ . Now, as  $\zeta \rightarrow 0$ ,

$$z \rightarrow -(i/\gamma)\mu^{1-\beta}\zeta^{-\gamma} + \text{constant},$$

so that

$$\bar{f} \rightarrow -\frac{1}{\theta_-} \log \left( -\frac{\gamma z}{i\mu^{1-\beta}} \right) + K.$$

This agrees with (3.2) if

$$\frac{1}{\theta_-} \log s = K + \frac{1}{\theta_-} \log \left( \frac{\mu^{1-\beta}}{\gamma} \right). \quad (\text{A8})$$

Similarly, as  $\zeta \rightarrow \infty$ ,

$$z \rightarrow -\frac{ie^{i\beta\pi}\pi}{\theta_+} \zeta^{\theta_+/\pi} + \text{constant},$$

so that

$$\bar{f} \rightarrow \frac{1}{\theta_+} \log \left( \frac{\theta_+ z}{-i\pi e^{i\beta\pi}} \right) + K,$$

which agrees with (3.2) if

$$-\frac{1}{\theta_+} \log s = K - \frac{1}{\theta_+} \log \left( \frac{\pi}{\theta_+} \right). \quad (\text{A9})$$

Subtraction of (A8) and (A9) to eliminate  $K$  yields the required formula for  $s$ , namely

$$\left( \frac{1}{\theta_+} + \frac{1}{\theta_-} \right) \log \frac{s}{\pi} = -\frac{1}{\theta_+} \log \theta_+ - \frac{1}{\theta_-} \log \theta_- + \frac{1}{\theta_-} \log(\mu^{1-\beta}),$$

or,

$$s = \pi \mu^{(1-\beta)\nu} \theta_+^{\nu-1} \theta_-^{-\nu}, \quad (\text{A10})$$

where

$$\nu = \theta_+ / (\theta_+ + \theta_-).$$

The problem is thus solved in an inverse manner, by prescribing  $\alpha$ ,  $\beta$ ,  $\gamma$ , and  $\mu$ . Results are wanted for  $s/w$ , where  $w = |z(-1)|$  is the throat width, that is, the distance between the corners  $H$  and  $D$ . Note that the length scale for the separate quantities  $s$  and  $w$  is arbitrarily set, by the choice of the mapping (A2), but this choice does not matter for their ratio  $s/w$ .

Results for  $\mu = 1$ ,  $\alpha = \beta$ , plotted against  $\theta_+$ , are shown in Figure 4 of the text. The solution given in this Appendix can be specialized to give many other important opening configurations. Cases with  $\alpha = \beta = 0$  correspond to thin walls at an arbitrary angle  $\pi\gamma$  to each other, as is the case for many breakwaters for harbour entrances. Cases with  $\beta = 1$  correspond to openings alongside a straight side wall.

**Appendix B: Derivation of rectangular cavity parameter**

The Fourier coefficients of equation (6.11) must be derived, as must the parameter  $b$ . The boundary condition  $\partial\phi_1/\partial x = 0$  on  $x = L$  is used to find  $a_n$  for  $n \neq 0$ .

The log term in (6.11) may be replaced by  $\Re\{\log(\sinh \pi(x + iy)/2h)\}$  to simplify the algebra. If we now differentiate (6.11) partially with respect to  $x$  at  $x = L$  and take the real part of  $\coth \pi/2h(L + iy)$  we obtain

$$\sum_{n=1}^{\infty} A_n \cos \frac{n\pi y}{h} = \frac{Lh}{\pi} \left( 1 - \frac{\sinh \frac{\pi L}{h}}{\cosh \frac{\pi L}{h} - \cos \frac{\pi y}{h}} \right) \tag{B1}$$

where

$$A_n = na_n \sinh \frac{n\pi L}{h}. \tag{B2}$$

Using the orthogonality of the cosine functions and converting the denominator of the right-hand side of (B1) to a geometric cosine series, (B1) can be written as

$$A_n = -\frac{2hL}{\pi^2} \tanh \frac{\pi L}{h} \sum_{j=0}^{\infty} \left( \cosh \frac{\pi L}{h} \right)^{-j} \int_0^{\pi} \cos^j \tau \cos n\tau d\tau \quad \text{for } n \geq 1. \tag{B3}$$

Thus, upon evaluation of the above integral (Gradshteyn and Ryzhik, [1], 3.63.17), the Fourier coefficients are determined.

To find,  $a_0$ , the normalization condition (5.7) is used, that is,

$$0 = -\frac{hL^3}{3} + 2a_0hL + \frac{2Lh}{\pi} \Re \left\{ \int_{-h}^h \int_0^L \log \left( \sinh \frac{\pi z}{2h} \right) dx dy \right\}. \tag{B4}$$

The integral in (B4), denoted  $I$ , is integrated by parts, and using the identity  $\partial/\partial x = -i(\partial/\partial y)$  we obtain

$$\frac{\pi I}{2Lh} = \Re \left\{ L \int_{-h}^h \log \left( \sinh \frac{\pi}{2h} (L + iy) \right) dy + i \int_0^L x \log \left( \frac{\sinh \frac{\pi}{2h} (x + ih)}{\sinh \frac{\pi}{2h} (x - ih)} \right) dx \right\}, \tag{B5}$$

which, upon expanding the hyperbolic functions in the second integral, becomes

$$\frac{\pi I}{2Lh} = \Re \left\{ L \int_{-h}^h \log \left( \sinh \frac{\pi}{2h} (L + iy) \right) dy \right\} - \frac{\pi L^2}{2}. \tag{B6}$$

Expanding the sinh in the remaining integral and taking the real part gives

$$\frac{\pi I}{2Lh} = -\frac{\pi L^2}{2} + \frac{hL}{\pi} \int_{-\pi/2}^{\pi/2} \log(a^2 - \cos^2 \tau) d\tau, \quad (\text{B7})$$

where  $a = \cosh \pi L/2h$ . Integrating by parts and using the definite integral

$$\int_0^{\pi/2} \frac{\tau \sin 2\tau}{1 + (-1/a^2)\cos^2 \tau} d\tau = -\pi a^2 \log\left(\frac{1 + \sqrt{1 - 1/a^2}}{2}\right) \quad (\text{B8})$$

(Gradshteyn and Ryzhik, [1], 3.81.2) gives

$$I = L^3 h. \quad (\text{B9})$$

Substituting (B9) back into (B4) we obtain  $a_0$ , namely

$$a_0 = -\frac{L^2}{3} + \frac{2hL}{\pi} \log 2. \quad (\text{B10})$$

To determine  $b$ , we use (6.3), the singularity condition at the origin. By letting  $(x, y) \rightarrow (0, 0)$  in (6.11) we find

$$\frac{1}{2\pi} \log \frac{r}{b} = \frac{1}{2\pi} \log\left(\frac{\pi}{2h} r\right) + \frac{1}{4hL} \sum_{n=0}^{\infty} a_n,$$

or,

$$b = \frac{2h}{\pi} \exp\left(-\frac{\pi}{2hL} \sum_{n=0}^{\infty} a_n\right). \quad (\text{B11})$$

## References

- [1] I. S. Gradshteyn and I. M. Ryzhik, *Tables of integrals, series and products* (Academic Press, New York, 4th edition, 1970).
- [2] H. von Helmholtz, "Theorie der Luftschwingungen in Röhren mit offenen Enden", *Crelle* 57 (1860), 1–72.
- [3] J.-J. Lee, "Wave induced oscillations in harbours of arbitrary shape", *Cal. Inst. Tech. W. M. Keck Lab. Hydraul. & Wat. Res. Rep. KH-R-20* (1969), 1–266.
- [4] J.-J. Lee, "Wave induced oscillations in harbours of arbitrary geometry", *J. Fluid Mech.* 45 (1971), 375–394.
- [5] J. W. Miles, "Resonant response of harbours: an equivalent-circuit analysis", *J. Fluid Mech.* 46 (1971), 241–265.
- [6] J. W. Miles, "Harbor seiching", *Annual Rev. Fluid Mech.* 6 (1974), 17–35.
- [7] J. W. Miles and Y. K. Lee, "Helmholtz resonance of harbours", *J. Fluid Mech.* 67 (1975), 445–464.
- [8] Lord Rayleigh, "On the theory of resonance", *Phil. Trans. Roy. Soc.* 161 (1870), 77–118.
- [9] Lord Rayleigh, *The theory of sound* (Dover, New York, 1945), Volume II.
- [10] E. O. Tuck, "Matching problems involving flow through small holes", *Adv. Appl Mech.* 15 (1974), 1–117.